Sputtered Tantalum Photonic Crystal Coatings for High-Temperature Energy Conversion Applications

Veronika Stelmakh, *Student Member, IEEE,* Walker R. Chan, Michael Ghebrebrhan, Jay Senkevich, John D. Joannopoulos, Marin Soljačić, and Ivan Celanović

***Abstract*—Recent advances in photonic crystals have enabled high-efficiency thermophotovoltaic (TPV) energy conversion by allowing near-perfect spectral control. In this work, photonic crystals fabricated in thick tantalum (Ta) coatings, sputtered onto a metallic substrate, were investigated as a potential replacement for photonic crystals fabricated in bulk refractory metal substrates in TPV applications. A 2D photonic crystal was fabricated in a 30 μm thick Ta sputtered coating using standard semiconductor processes as a proof-of-concept for a selective emitter / solar absorber. The reflectance of the fabricated photonic crystal coating was characterized before and after one-hour anneals at 700, 900, and 1100°C, and after a 24 hour anneal at 900°C. To protect its surface during the anneals, a thin conformal hafnia (HfO_2) layer was deposited by atomic layer deposition on the photonic crystal. The photonic crystal showed high spectral selectivity in good agreement with numerical simulations and sustained the anneals with minimal structural degradation or change in its optical properties. This study presents a promising alternative to bulk substrates as a relatively low-cost and easily integrated platform for nano-structured devices in high-temperature energy conversion systems.**

***Index Terms*—Thermophotovoltaics, photonic crystal, high-temperature coatings, energy conversion.**

I. Introduction

Thermophotovoltaic (TPV) energy conversion is a high-temperature heat-to-electricity conversion scheme with no moving parts that allows for scalable energy production with high power density from a variety of heat sources. In TPV systems, thermal radiation from a heat source at high temperature drives a suitable low-bandgap photovoltaic cell (PV). The heat can be produced by hydrocarbon combustion, ideal for lightweight, high specific energy portable power sources [1]–[3]; by radioisotope decay, ideal for space missions and remote missions requiring power sources with long lifetimes and low maintenance [4]; or by concentrated solar radiation [5]. High-efficiency TPV energy conversion has only recently been enabled by advances in photonic crystals, which allow near perfect spectral control. These photonic crystals can be designed as selective emitters, as well as solar absorbers, or a combined emitter/absorber pair, as shown in Fig. 1.

V. Stelmakh, W. Chan, J. Senkevich, M. Soljačić, J. Joannopoulos, and I. Celanović are with the Institute for Soldier Nanotechnologies, Massachusetts Institute of Technology, Cambridge, Massachusetts 02139 USA email: stelmakh@mit.edu.

M. Soljačić and J. Joannopoulos are additionally with the Department of Physics, Center for Materials Science and Engineering, and Research Laboratory of Electronics, Massachusetts Institute of Technology, Cambridge, Massachusetts 02139 USA.

M. Ghebrebrhan is with the U.S. Army Natick Soldier Research, Development, and Engineering Center, Natick, Massachusetts 01760, USA.

978-1-4673-8156-7/15/$31.00 2015 IEEE

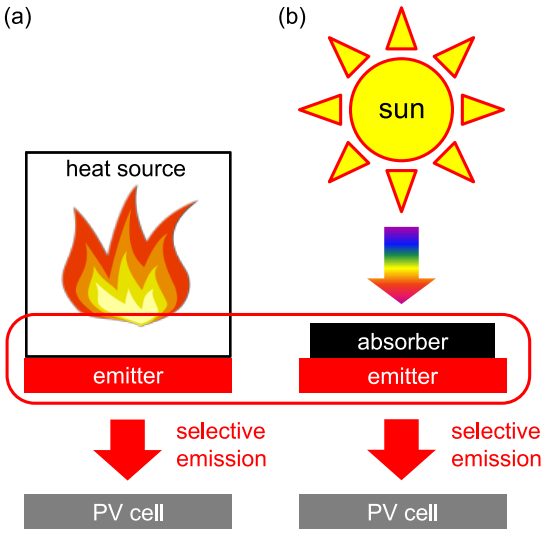

Fig. 1. Simplified schematic of TPV high-temperature energy conversion schemes. (a) In a TPV system, a source of heat (such as a hydrocarbon-fueled microburner or radioisotope general purpose heat source) brings an emitter to incandescence by direct thermal contact. (b) In a solar TPV system, concentrated solar radiation heats a selective absorber, maximizing the solar absorptance, in thermal contact with a selective emitter. In all TPV systems, the radiation from the emitter is then incident on a low-bandgap PV cell. The selective emitter enables higher system efficiencies by matching the emission spectrum to the response of the PV cell.

A selective emitter enables a higher heat-to-electricity conversion efficiency by producing spectrally confined selective emission of light matching the bandgap of the PV cell [6]–[8]. As shown in Fig. 2(a), only a small portion of the radiation of a blackbody emitter falls within the convertible (in-band) range of a low-bandgap PV cell. The radiation that falls outside of this region (out-of-band) is wasted. Substituting a 2D photonic crystal instead of a graybody emitter with 0.9 emissivity in a TPV system using an InGaAsSb PV cell (which has a bandgap $E_g = 0.53$ eV corresponding to a cutoff wavelength $\lambda_{PV} = 2.3$ μm) would reduce the out-of-band radiation by about half and increase the overall heat-to-electricity efficiency from 7.5% to 13% [9].

A solar absorber enables higher net absorption by maximizing the solar absorptance while simultaneously minimizing the thermal radiation by wavelength-dependent emissivity, as shown in Fig. 2(b). Selective solar photonic crystal absorbers have been shown to improve solar TPV system efficiency by a factor of 2.3 compared to a blackbody absorber, using a similar 2D photonic crystal emitter design matched to an InGaAsSb cell [10].

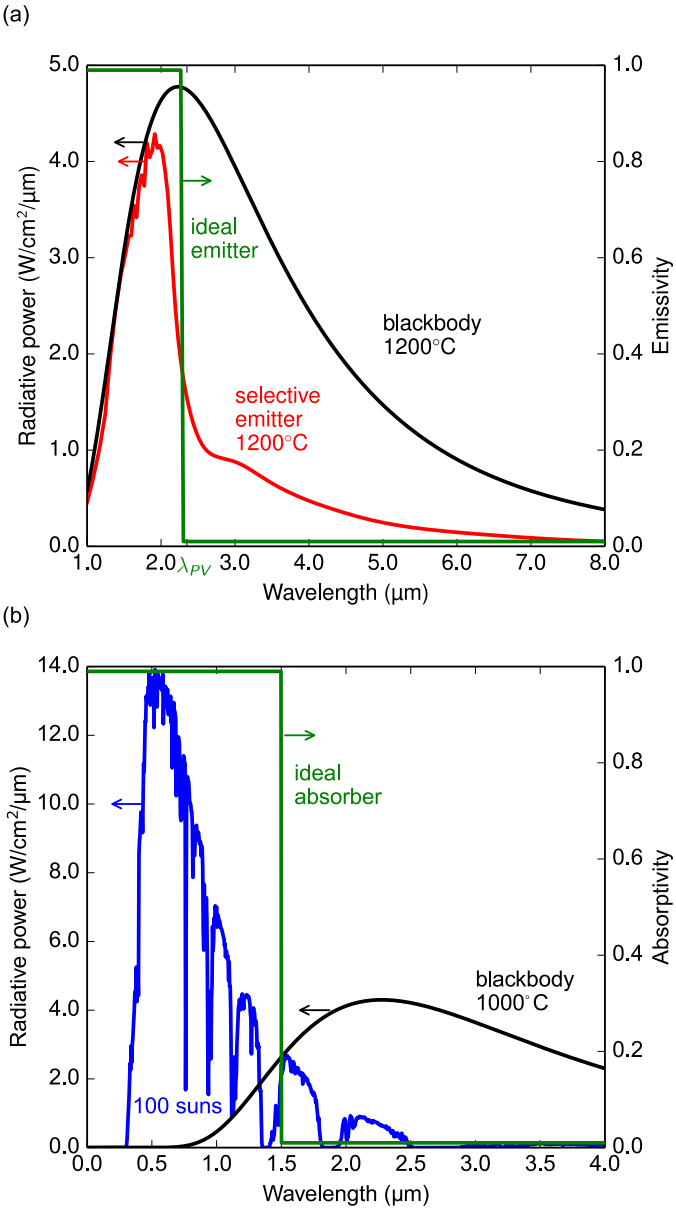

Fig. 2. (a) A selective emitter enables higher system efficiencies by matching the emission spectrum (shown at 1200°C in red) to the response of a low-bandgap photovoltaic cell, in this case an InGaAsSb cell. A blackbody at 1200°C (shown in black for comparison) has more than half of its emission outside of the in-band region. (b) A solar absorber maximizes absorptance of the incident spectrum (AM1.5, 100X sun concentration, shown in blue) while simultaneously minimizing the thermal radiation, shown as a blackbody (in black) at 1000°C, by wavelength-dependent emissivity. An ideal emitter/absorber has a step function emissivity/absorptivity, equal to one below the cutoff and equal to zero above the cutoff wavelength.

Photonic crystals fabricated as 1D, 2D, and 3D structures or metamaterials [11]–[16] enable higher system efficiencies by tailoring the photonic density of states to produce spectrally confined selective emission of light [6], [7], [17]. Microstructured 2D photonic crystal thermal emitters and absorbers have been fabricated on single-crystal tungsten (W) bulk substrates [6], [7], [11], [13], [14], as well as on polycrystalline Ta and Ta-W alloy bulk substrates [8], [18], by etching a periodic pattern into the low-emissivity (i.e., high reflectivity) polished metallic substrate. Refractory metals, such as Ta and W, are most suitable for high-temperature (∼900–1200°C) energy conversion applications due to their high melting point, low vapor pressure, low infrared emissivity, and ability to be etched. However refractory metals are notoriously difficult to machine and weld, which is detrimental for system integration.

Indeed, once the photonic crystal is fabricated, the challenge remains to integrate it into a compact system operating at high temperatures. In hydrocarbon and radioisotope TPV applications, spectral components fabricated from bulk substrates add weight to the system and must be welded onto the heat source, for example an Inconel microburner [19]. A TPV emitter directly integrated into the system in the form of a coating requires less material, decreases the fabrication complexity, reduces the integration cost, and reduces undesirable parasitic edge radiation from having reduced thickness. Using a Ta coating as a functional layer on different substrates, selected and matched to the system's needs, decouples the requirements of the functional layer and the substrate.

Previously, sputtered W coatings and their evolution at high temperatures were studied as a potential fabrication route for high-temperature nano-structured surfaces [20]. This study revealed that sputtered W layers were a promising approach for a photonic crystal substrate, if the challenge of delamination at high temperatures could be overcome. In another study, evaporated thin Ta coatings were found to have low film density and high surface roughness, resulting in high emittance in the near-infrared wavelength range, which made them unsuitable as a photonic crystal substrate [21]. In our most recent study, thick Ta coatings were sputtered on polished Inconel 625, which is a readily available low-cost nickel-chromium-based superalloy used in many high-temperature applications [22]. The non-structured coatings were characterized before and after anneal and were found to be suitable substrates for high-temperature energy conversion applications, showing no noticeable deterioration of either the optical or thermo-mechanical properties after annealing at temperatures up to 1100°C.

Using the 30 μm sputtered Ta coating characterized in our previous study as the substrate, a 2D photonic crystal selective emitter was fabricated by interference lithography and reactive ion etching. The selective emitter was designed for a TPV system using a GaSb TPV cell with a bandgap corresponding to a cutoff wavelength of 1.7 μm. A conformal layer of hafnia (HfO_2) was deposited as a protective barrier coating for high-temperature stability. The optical performance of the photonic crystal was characterized and compared with simulations, before and after anneals in vacuum at 700, 900, and 1100°C. No damage, such as cracking or delamination,

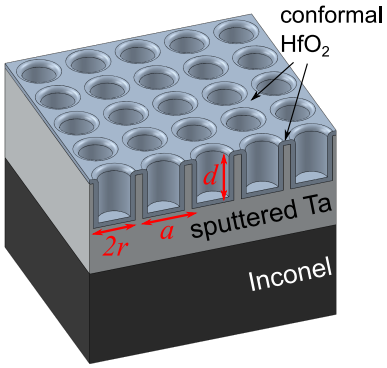

Fig. 3. The fabricated 2D photonic crystal consisted of a square array of cylindrical cavities with radius r, period a, and depth d, etched into the sputtered Ta to selectively enhance the spectral emissivity in a given spectral range. A conformal coating of hafnia was deposited after the photonic crystal was fabricated to enhance its thermal stability at high temperatures.

in the surface or microstructure was observed from visual inspection of micrographs after anneal. The optical properties of the selective emitter remained remarkably stable even after annealing for 24 hours at 900°C. Overall, the results of this study suggest that thick Ta coatings are a promising alternative to bulk substrates as a relatively low-cost and easily integrated platform for nano-structured devices in high-temperature energy conversion systems.

II. Photonic Crystal Design, Fabrication, and Characterization

A. Photonic Crystal Design

The fabricated 2D photonic crystal consisted of a square array of cylindrical cavities with radius r, period a, and depth d etched into the sputtered Ta, as shown in Fig. 3, to selectively enhance the spectral emissivity in a certain spectral range by introducing cavity resonances. The geometric parameters (r, a and d) were chosen to match a specific cutoff wavelength with both finite-difference time domain and rigorous coupled wave simulations [23], [24]. The dispersion of bulk and sputtered Ta at room and elevated temperatures were captured via a Lorentz-Drude model. Qualitatively, the higher absorbance of sputtered Ta at near-IR wavelengths compared to bulk Ta results in slightly wider and more shallow cavities than in bulk Ta. From a Q-matching point-of-view, the higher material absorption will result in a lower absorptive Q. The radiative Q, which scales as $(d/r)^3$, can match the absorptive Q if r increases and d decreases [17]. In addition the optimal radius, less than the skin depth, will be determined by the waveguide cutoff and wavelength of interest, i.e., $r \approx 1.8412 * \lambda_{PV}/(2\pi)$. The addition of the thin conformal hafnia coating will pull down the waveguide cutoff frequency and to compensate, the radius should be decreased. The hafnia coating will also slightly increase the density of cavity states though not to the extent as completely plugging the cavity [25], [26]. Here, thermo-mechanical considerations were more important in determining the hafnia coating thickness.

Our 2D photonic crystal was designed for a cutoff at 1.7 μm as a proof-of-concept for a selective emitter. However the cutoff wavelength can be easily tuned for different cutoffs by altering the geometric parameters, especially the cavity radius. In addition to tuning the geometric parameters, the cutoff can be further fine-tuned by the thickness of the conformal hafnia layer.

B. Sputtered Coating Fabrication

The fabrication and charaterization of the sputtered coatings is detailed in Ref. [22]. Tantalum coatings were fabricated via ion-assisted DC magnetron sputtering on Inconel 625 2×2 cm substrates. Inconel was used as it is a readily available low-cost nickel-chromium-based superalloy used in combustion TPV applications. A deposition temperature of 300°C at 2 kW was used. Argon (Ar) was used as the sputtering gas and the vacuum chamber pressure was 2 mTorr with a base pressure of 5×10^{-6} Torr. A 40 V bias was applied on the samples and the discharge filament was run at 40 A for the secondary plasma to increase ion bombardment. The thicknesses of the Ta sputtered layer was determined by contact profilometry after deposition and found to be 30 μm via witness coupons. The coatings were thoroughly characterized by X-ray diffraction (XRD), atomic force microscopy (AFM), and optical measurements. From XRD analysis, the Ta sputtered coatings were found to be in a state of compressive stress, thereby producing dense coatings with high reflectivity. Indeed, the reflectance of the thick coatings was found to be exceptionally high as-deposited and comparable to that of polished bulk samples, even after anneal. Analysis by AFM confirmed that no significant change in roughness was observed, as expected from the reflectance measurements, thus meeting the roughness and reflectance requirements for thermal emitters. Furthermore, annealing the coatings was not found to produce any significant changes in the residual stress, demonstrating that phenomena such as plastic deformation, phase transformations, grain growth, and oxidation were not significant under these conditions.

C. Photonic Crystal Fabrication

The photonic crystal fabrication process for the sputtered Ta substrates was similar to the one developed previously for bulk Ta substrates using interference lithography and reactive ion etching (RIE) of a hard mask and a subsequent deep RIE (DRIE) of the Ta [18], [27]. A 200 nm layer of silicon dioxide (SiO_2) was deposited by plasma-enhanced chemical vapor deposition (PECVD) onto the cleaned substrates to be used as a hard mask for the Ta etching. An anti-reflection coating (ARC, AZ BARLi) of about 270 nm was then spin-coated and another 10 nm layer of SiO_2 was electron-beam evaporated onto the sample. The SiO_2 layer on top of the ARC served as a protection layer when etching and ashing the ARC. Finally, a layer of about 250 nm of negative photoresist (THMR-iNPS4, OHKA America) was spin-coated onto the sample for the lithography process. Interference lithography was performed using a Mach-Zehnder setup with a 325 nm helium cadmium (HeCd) laser to obtain a large periodic pattern with high uniformity. The square array of cylindrical holes was created by double exposure of the photoresist and the cavity diameter was enlarged to the desired value by isotropic plasma ashing.

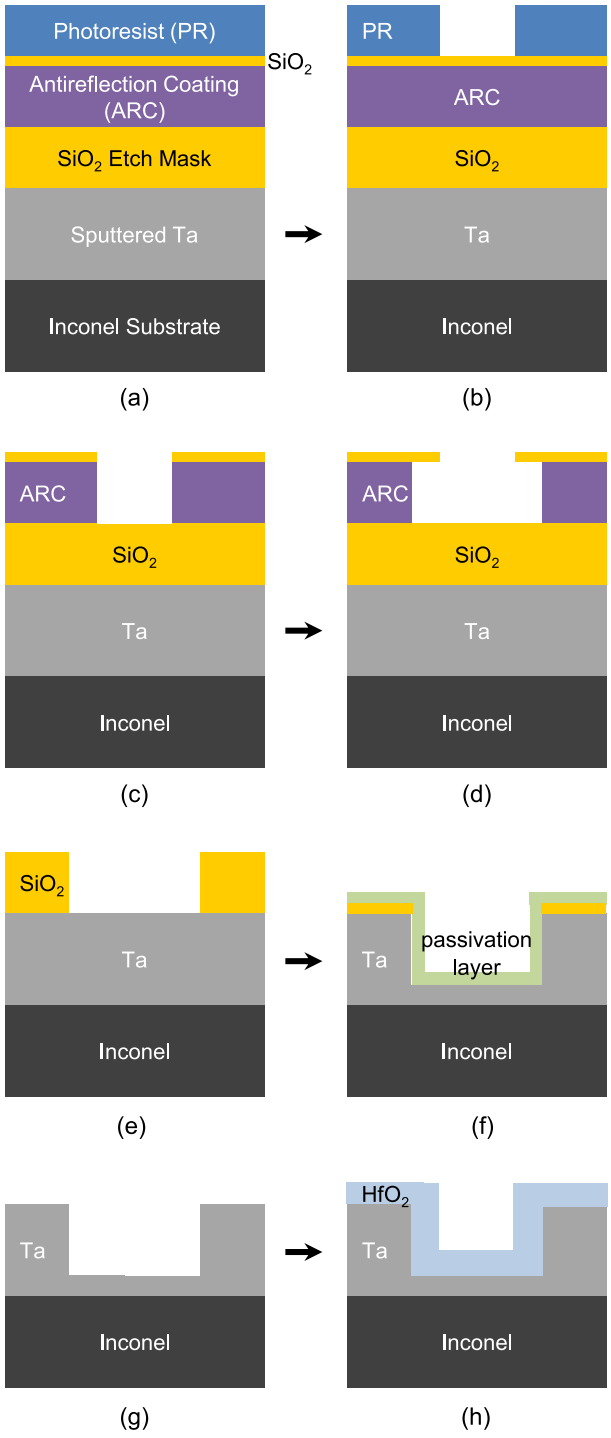

Fig. 4. A general process flow for the fabrication of our 2D photonic crystal involves: pattern generation, pattern transfer into a hard mask by etching, pattern transfer into the metallic substrate by etching, and surface passivation for thermal stability. The fabrication process is shown here in a cross-section schematic: (a) trilayer stack deposition, (b) photoresist exposure and development, (c) pattern transfer by RIE, (d) cavity radius opening by O_2 plasma ashing, (e) RIE of etch mask, (f) DRIE of Ta by Bosch etch process, showing fluorcarbon passivation layer (g) removal of residual layers by plasma ashing and HF, and (h) hafnia protective layer deposition by ALD.

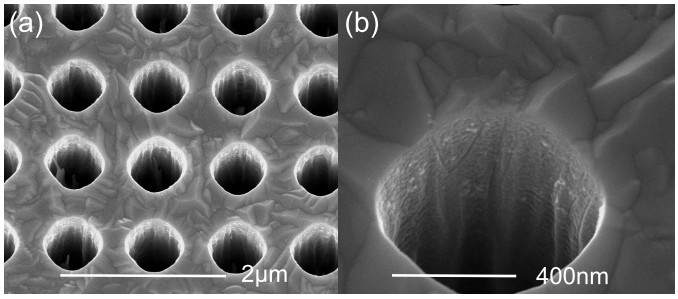

Fig. 5. Micrographs of the photonic crystal fabricated in the Ta sputtered coating, before the hafnia conformal coating deposition and before annealing.

The pattern was subsequently transferred into the SiO_2 mask by RIE. The final etching of the Ta substrate was done by a Bosch DRIE process using sulfur hexafluoride (SF_6) and octafluorocyclobutane (C_4F_8) as the etching and passivating gaseous species. The residual passivation layer was removed by oxygen (O_2) ashing and the residual SiO_2 layer was removed by hydrofluoric acid (HF). A conformal layer of hafnia was deposited via atomic layer deposition (ALD) at 250°C, using tetrakis dimethylamino hafnium (TDMAH) and water as precursors, to prevent degradation of the coatings at high temperatures [28].

D. Photonic Crystal Characterization

The fabricated 2D photonic crystal sputtered Ta coating was measured by scanning electron microscopy (SEM) and found to have a period $a \approx 1$ μm, radius $r \approx 0.3$ μm, and cavity depth $d \approx 3$ μm, as shown in Fig. 5.

The spectral emissivity at room temperature was obtained by measuring near-normal incidence reflectance using an automated spectroradiometric measurement system (Gooch & Housego OL750). A sharp cutoff was observed in the desired wavelength range. The in-band emittance was increased to almost the blackbody limit, while the out-of-band emittance approached the emissivity of flat Ta. The measured emittance of the photonic crystal was matched to the simulated (room temperature) emittance, and was found to be in best agreement with $a = 1.01$ μm, $r = 0.35$ μm, and $d = 2.5$ μm, as shown in Fig. 6(a).

The cutoff wavelength was measured to be 1.65 μm, which is very close to the bandgap of a GaSb TPV cell. The emittance of the fabricated sputtered photonic crystal emitter after the conformal hafnia coating deposition is shown in Fig. 6(a) compared to the emittance of an emitter fabricated in bulk Ta tuned for a similar cutoff wavelength, as well as the simulated emittance for the sputtered photonic crystal coating. The selective emitter previously fabricated in bulk Ta had an average normal in-band emittance of 97.6% and average normal out-of-band emittance of 18.1%. The average normal in-band emittance of our fabricated sputtered photonic crystal was found to be 84.5% and the average normal out-of-band emittance was found to be 12.7%. Thus, this is a very promising initial performance for a sputtered 2D photonic crystal selective emitter for high-temperature applications.

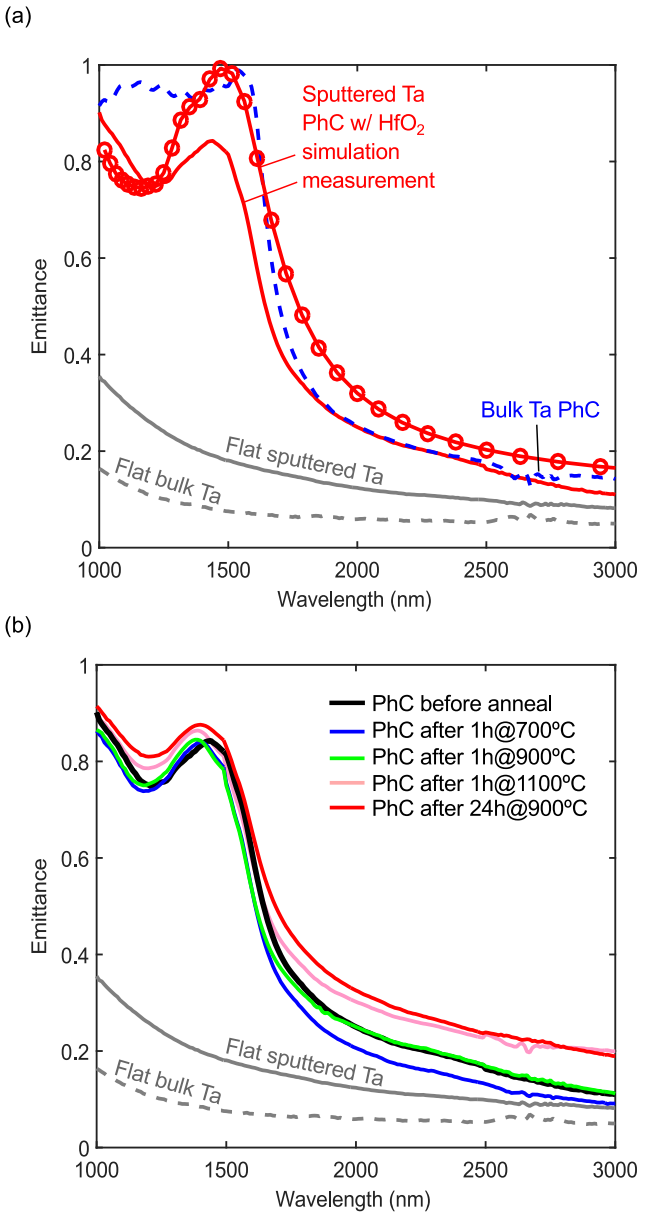

Fig. 6. (a) Emittance of the fabricated sputtered 2D photonic crystal coating after conformal hafnia deposition compared to the flat (as deposited) sputtered Ta coating, flat (as received) bulk polished Ta, and photonic crystal simulation (room temperature Ta emissivity, $a = 1.01$ μm, $r = 0.35$ μm, and $d = 2.5$ μm, coated). (b) Emittance of the fabricated sputtered 2D photonic crystal coating after the conformal hafnia deposition before and after annealing compared to the flat (as deposited) sputtered Ta coating, and flat (as received) bulk polished Ta.

In order to characterize the optical properties as a function of temperature, the photonic crystal coating was annealed for one hour at 700, 900, and 1100°C and 24 hours at 900°C in a quartz-lined Inconel tube furnace in vacuum (5×10^{-6} Torr), at a slow heating and cooling rate of 5°C/minute. The emittance of the selective emitter fabricated in the hafnia coated 30 μm Ta coating before and after the anneals was characterized, as shown in Fig. 6(b), and compared to the flat sputtered coating and flat bulk Ta, measured at room temperature. The optical properties of the selective emitter remained remarkably stable even after annealing for 24 hours at 900°C. No damage, such as cracking or delamination, in the surface or microstructure was observed from visual inspection of micrographs after annealing. These results are very promising and lay a foundation for a relatively low-cost and easily integrated platform for nanostructured devices for high-temperature applications.

III. System Performance Improvement

In a TPV system, as previously discussed, a high temperature heat source (combustion, radioactive decay, concentrated sunlight) heats the photonic crystal to incandescence and the resulting thermal radiation is converted by low-bandgap PV cells. In order to evaluate the performance of selective emitters, we define two figures of merit: spectral efficiency and in-band emissivity. Spectral efficiency, the fraction of input heat converted to in-band radiation, largely determines the heat-to-electricity conversion efficiency. In-band emissivity, the total in-band power normalized to the blackbody, determines the required active area to achieve a specified electrical power output and is important in calculating the overall (for example, fuel-to-electricity) conversion efficiency for a lossy system where in-band thermal radiation must compete with other heat loss mechanisms (exhaust, parasitic radiation, etc). Mathematically, the spectral efficiency η_{sp} and in-band emissivity ε_{in} are defined as:

$$\eta_{sp} = \frac{\int_0^{\lambda_{PV}} \varepsilon(\lambda)\, e_b(\lambda)\, d\lambda}{\int_0^{\infty} \varepsilon(\lambda)\, e_b(\lambda)\, d\lambda} \tag{1}$$

$$\varepsilon_{in} = \frac{\int_0^{\lambda_{PV}} \varepsilon(\lambda)\, e_b(\lambda)\, d\lambda}{\int_0^{\lambda_{PV}} e_b(\lambda)\, d\lambda} \tag{2}$$

where $\varepsilon(\lambda)$ is the emitter's hemispherically-averaged wavelength-dependent emissivity, $e_b = 2hc^2/[\lambda^5(e^{hc/\lambda k_B T} - 1)]$ is the Planck blackbody, λ is the wavelength, λ_{PV} corresponds to the bandgap of the PV cell (in our case, $\lambda_{PV} = 1.7$ μm for GaSb), h is Planck's constant, c is the speed of light, k_B is the Boltzmann constant, and T is the emitter temperature.

The calculated spectral efficiency and in-band emissivity for the photonic crystal emitter, flat Ta, and a blackbody are presented in Fig. 7. The emissivity used in the calculations was hemispherically averaged over all polar and azimuthal angles to account for angular dependence inherent in the photonic crystal structure. Furthermore, the high temperature material properties were used to simulate the actual performance of a real TPV system. The spectral efficiency increases with temperature because the blackbody spectrum shifts to shorter wavelengths, thus increasing the in-band fraction. Temperature alone cannot be used to achieve high spectral efficiency because of material stability limitations and because increased heat loss elsewhere in the system counteracts gains in spectral efficiency. On the other hand, the in-band emissivity remains nearly constant with temperature because the material properties do not change much with temperature.

The spectral efficiency and in-band emissivity is shown for two emitter temperatures (1200°C and 1500°C) in Table I. The spectral efficiency of the photonic crystal is approximately double that of a blackbody because of the reduced out-of-band

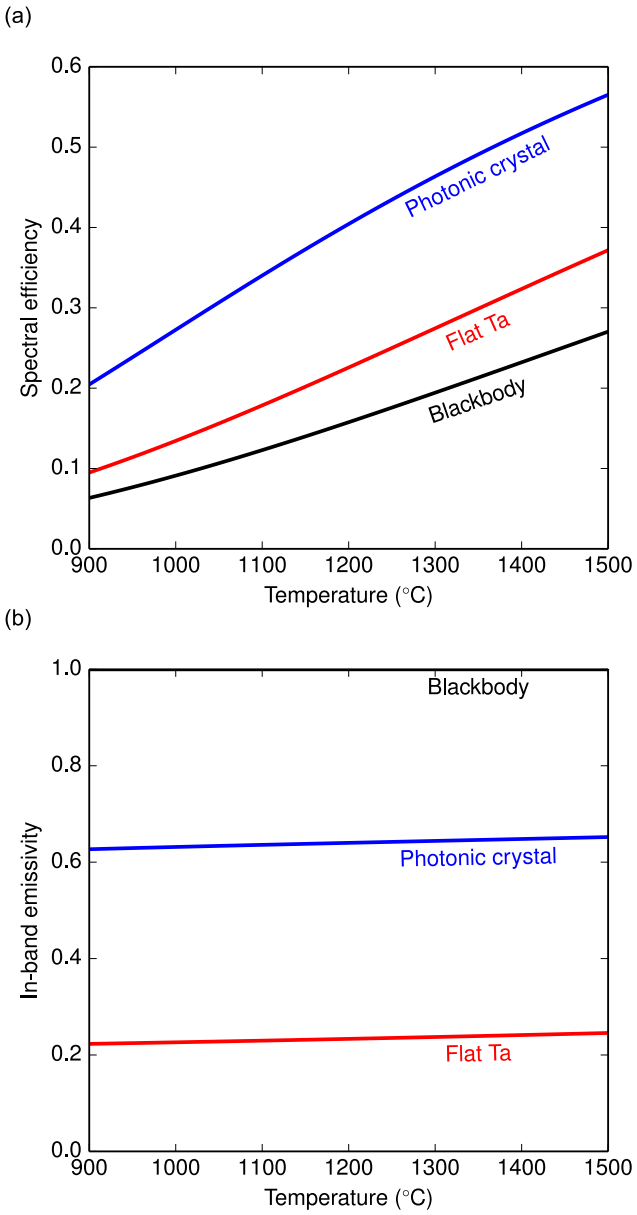

Fig. 7. (a) Calculated spectral efficiency and (b) in-band emissivity of the 2D sputtered Ta photonic crystal emitter, flat polished Ta emitter, and blackbody emitter for λ_{PV}=1.7 μm, as a function of temperature.

TABLE I
SPECTRAL EFFICIENCY AND IN-BAND EMISSIVITY OF DIFFERENT EMITTERS.

	Spectral efficiency		In-band emissivity	
Emitter type	1200°C	1500°C	1200°C	1500°C
Sputtered 2D PhC	0.404	0.565	0.640	0.652
Flat Ta	0.226	0.372	0.233	0.246
Blackbody	0.158	0.270	1.000	1.000

radiation. The photonic crystal achieves an in-band emissivity about 65% of the blackbody limit. The in-band emissivity can be further increased towards the blackbody limit by optimizing the geometry to maximize hemispherical emission [25].

IV. Conclusion

We fabricated and characterized a 2D photonic crystal in a sputtered Ta coating on Inconel for use as a selective emitter in a monolithic TPV system. The spectral efficiency and in-band irradiance of the fabricated selective emitter was found to be approximately double that of the non-structured surface. The high temperature stability of the fabricated photonic crystal was tested by annealing for one hour at 700, 900, and 1100°C, and for 24 hours at 900°C. No delamination, surface deterioration, or microstructural damage was observed from visual inspection of micrographs. Minimal degradation of the optical spectrum was observed. These results pave the way for a new integration path of the selective emitter in thermophotovoltaic energy conversion applications. Furthermore, our 2D photonic crystal design can be easily tuned to match the optimized cutoff wavelength for a given system, and can also be easily designed as a solar absorber. Overall, the results of this study suggest that thick Ta coatings are a promising alternative to bulk substrates as a relatively low-cost and easily integrated platform for nano-structured devices in high-temperature energy conversion systems.

Acknowledgment

The authors would like to thank: R. Geil at the University of North Carolina at Chapel Hill for DRIE of Ta; J. Daley and T. Savas at NSL (MIT) for assitance with film deposition and interference lithography; R. Wei, R. Castillo, and K. Coulter at Southwest Research Institute for Ta sputtering; L. Gibbons at H.C. Starck for waterjetting of the Inconel substrates; and V. Rinnerbauer for insightful discussions. Fabrication was done in part at the Nanostructures Laboratory (NSL) at MIT and at the Center for Nanoscale Systems (CNS) at Harvard University, a member of the National Nanotechnology Infrastructure Network (NNIN), supported by the National Science Foundation (NSF) under NSF Award No. ECS-0335765. Fabrication was supported by the Solid-State Solar-Thermal Energy Conversion Center (S3TEC), an Energy Frontier Research Center funded by the U.S. Department of Energy (DOE), Office of Science, Basic Energy Sciences (BES), under Award # DE-SC0001299 / DE-FG02-09ER46577. Research was also supported by the U.S. Army Research Laboratory and the U.S. Army Research Office through the Institute for Soldier Nanotechnologies, under Contract # W911NF-13-D-0001.

References

[1] E. Doyle, K. Shukla, and C. Metcalfe, "Development and Demonstration of a 25 Watt Thermophotovoltaic Power Source for a Hybrid Power System," National Aeronautics and Space Administration, Tech. Rep. TR04-2001, 2001.

[2] B. Bitnar, W. Durisch, and R. Holzner, "Thermophotovoltaics on the move to applications," *Applied Energy*, vol. 105, pp. 430–438, 2013.

[3] W. R. Chan, P. Bermel, R. C. N. Pilawa-Podgurski, C. H. Marton, K. F. Jensen, J. J. Senkevich, J. D. Joannopoulos, M. Soljacic, and I. Celanovic, "Toward high-energy-density, high-efficiency, and moderate-temperature chip-scale thermophotovoltaics," *Proceedings of the National Academy of Sciences*, vol. 110, no. 14, pp. 5309–5314, 2013.

[4] C. J. Crowley, N. a. Elkouh, S. Murray, and D. L. Chubb, "Thermophotovoltaic converter performance for radioisotope power systems," *AIP Conference Proceedings*, vol. 746, no. 2005, pp. 601–614, 2005.

[5] A. Lenert, D. M. Bierman, Y. Nam, W. R. Chan, I. Celanovic, M. Soljačić, and E. N. Wang, "A nanophotonic solar thermophotovoltaic device," *Nature Nanotechnology*, vol. 9, no. January, pp. 1–5, 2014.

[6] H. Sai, Y. Kanamori, and H. Yugami, "High-temperature resistive surface grating for spectral control of thermal radiation," *Appl. Phys. Lett.*, vol. 82, pp. 1685–1687, 2003.

[7] Y. X. Yeng, M. Ghebrebrhan, P. Bermel, W. R. Chan, J. D. Joannopoulos, M. Soljacic, and I. Celanovic, "Enabling high-temperature nanophotonics for energy applications," *Proceedings of the National Academy of Sciences*, vol. 109, no. 7, pp. 2280–2285, 2012.

[8] V. Rinnerbauer, S. Ndao, Y. X. Yeng, W. R. Chan, J. J. Senkevich, J. D. Joannopoulos, M. Soljačić, and I. Celanovic, "Recent developments in high-temperature photonic crystals for energy conversion," *Energy & Environmental Science*, vol. 5, no. 10, p. 8815, 2012.

[9] Y. X. Yeng, W. R. Chan, V. Rinnerbauer, J. D. Joannopoulos, and I. Celanovic, "Performance analysis of experimentally viable photonic crystal enhanced thermophotovoltaic systems," *Optics Express*, vol. 21, no. S6, pp. 2879–2891, 2013.

[10] V. Rinnerbauer, A. Lenert, D. M. Bierman, Y. X. Yeng, W. R. Chan, R. D. Geil, J. J. Senkevich, J. D. Joannopoulos, E. N. Wang, M. Soljačić, and I. Celanovic, "Metallic photonic crystal absorber-emitter for efficient spectral control in high-temperature solar thermophotovoltaics," *Advanced Energy Materials*, vol. 4, no. 12, p. 1400334, 2014.

[11] A. Heinzel, V. Boerner, A. Gombert, B. Blasi, V. Wittwer, and J. Luther, "Radiation filters and emitters for the NIR based on periodically structured metal surfaces," *J. Mod. Opt.*, vol. 47, 2000.

[12] H. Sai and H. Yugami, "Thermophotovoltaic generation with selective radiators based on tungsten surface gratings," *Applied Physics Letters*, vol. 85, no. 16, pp. 3399–3401, 2004.

[13] E. Rephaeli and S. Fan, "Tungsten black absorber for solar light with wide angular operation range," *Applied Physics Letters*, vol. 92, no. 21, p. 211107, 2008.

[14] I. Celanovic, N. Jovanovic, and J. Kassakian, "Two-dimensional tungsten photonic crystals as selective thermal emitters," *Applied Physics Letters*, vol. 92, no. 19, p. 193101, 2008.

[15] K. A. Arpin, M. D. Losego, and P. V. Braun, "Electrodeposited 3D tungsten photonic crystals with enhanced thermal stability," *Chemistry of Materials*, vol. 23, no. 21, pp. 4783–4788, 2011.

[16] P. Nagpal, D. P. Josephson, N. R. Denny, J. DeWilde, D. J. Norris, and A. Stein, "Fabrication of carbon/refractory metal nanocomposites as thermally stable metallic photonic crystals," *Journal of Materials Chemistry*, vol. 21, no. 29, p. 10836, 2011.

[17] M. Ghebrebrhan, P. Bermel, Y. X. Yeng, I. Celanovic, M. Soljacic, and J. D. Joannopoulos, "Tailoring thermal emission via Q matching of photonic crystal resonances," *Physical Review A - Atomic, Molecular, and Optical Physics*, vol. 83, no. 3, pp. 1–6, 2011.

[18] V. Stelmakh, V. Rinnerbauer, R. D. Geil, P. R. Aimone, J. J. Senkevich, J. D. Joannopoulos, M. Soljačić, and I. Celanovic, "High-temperature tantalum tungsten alloy photonic crystals: Stability, optical properties, and fabrication," *Applied Physics Letters*, vol. 103, no. 12, 2013.

[19] W. R. Chan, B. A. Wilhite, J. J. Senkevich, M. Soljacic, J. D. Joannopoulos, and I. Celanovic, "An all-metallic microburner for a millimeter-scale thermophotovoltaic generator," in *Journal of Physics: Conference Series*, vol. 476, no. 1, 2013, p. 012017.

[20] V. Stelmakh, V. Rinnerbauer, J. D. Joannopoulos, M. Soljacic, I. Celanovic, J. J. Senkevich, C. Tucker, T. Ives, R. Shrader, M. Soljacic, I. Celanovic, J. J. Senkevich, C. Tucker, T. Ives, and R. Shrader, "Evolution of sputtered tungsten coatings at high temperature," *Journal of Vacuum Science & Technology A: Vacuum, Surfaces, and Films*, vol. 31, no. 6, p. 061505, 2013.

[21] V. Rinnerbauer, J. J. Senkevich, J. D. Joannopoulos, M. Soljacic, I. Celanovic, R. R. Harl, B. R. Rogers, M. Soljacic, I. Celanovic, R. R. Harl, and B. R. Rogers, "Low emissivity high-temperature tantalum thin film coatings for silicon devices," *Journal of Vacuum Science & Technology A: Vacuum, Surfaces, and Films*, vol. 31, no. 1, p. 011501, 2013.

[22] V. Stelmakh, D. Peykov, W. R. Chan, J. J. Senkevich, J. D. Joannopoulos, M. Soljačić, I. Celanovic, R. Castillo, K. Coulter, and R. Wei, "Thick sputtered tantalum coatings for high-temperature energy conversion applications," *Journal of Vacuum Science & Technology A*, vol. 33, no. 6, 2015.

[23] A. F. Oskooi, D. Roundy, M. Ibanescu, P. Bermel, J. D. Joannopoulos, and S. G. Johnson, "Meep: A flexible free-software package for electromagnetic simulations by the FDTD method," *Computer Physics Communications*, vol. 181, no. 3, pp. 687–702, 2010.

[24] V. Liu and S. Fan, "S 4: A free electromagnetic solver for layered periodic structures," *Computer Physics Communications*, vol. 183, no. 10, pp. 2233–2244, 2012.

[25] J. B. Chou, Y. X. Yeng, A. Lenert, V. Rinnerbauer, I. Celanovic, M. Soljačić, E. N. Wang, and S.-G. Kim, "Design of wide-angle selective absorbers/emitters with dielectric filled metallic photonic crystals for energy applications." *Optics express*, vol. 22 Suppl 1, no. January, pp. A144–54, 2014.

[26] Y. X. Yeng, J. B. Chou, V. Rinnerbauer, Y. Shen, S.-G. Kim, J. D. Joannopoulos, M. Soljačić, I. Celanovic, M. Soljacic, I. Celanovic, and I. Čelanović, "Global optimization of omnidirectional wavelength selective emitters/absorbers based on dielectric-filled anti-reflection coated two-dimensional metallic photonic crystals," *Optics Express*, vol. 22, no. 18, p. 21711, 2014.

[27] V. Rinnerbauer, S. Ndao, Y. Xiang Yeng, J. J. Senkevich, K. F. Jensen, J. D. Joannopoulos, M. Soljacic, I. Celanovic, R. D. Geil, M. Soljacic, I. Celanovic, and R. D. Geil, "Large-area fabrication of high aspect ratio tantalum photonic crystals for high-temperature selective emitters," *Journal of Vacuum Science & Technology B: Microelectronics and Nanometer Structures*, vol. 31, no. 1, p. 11802, 2013.

[28] V. Rinnerbauer, Y. X. Yeng, W. R. Chan, J. J. Senkevich, J. D. Joannopoulos, M. Soljačić, and I. Celanovic, "High-temperature stability and selective thermal emission of polycrystalline tantalum photonic crystals." *Optics express*, vol. 21, no. 9, pp. 11 482–91, May 2013.